# Autonomous and forced dynamics of oscillator ensembles with global nonlinear coupling: An experimental study

Amirkhan A. Temirbayev,[1] Yerkebulan D. Nalibayev,[1] Zeinulla Zh. Zhanabaev,[1]
Vladimir I. Ponomarenko,[2] and Michael Rosenblum[3]
[1]*Physical-Technical Department, al-Farabi Kazakh National University, al-Farabi Avenue 71, 050040 Almaty, Kazakhstan*
[2]*Institute of Radio Engineering and Electronics, Saratov Branch, Russian Academy of Sciences, 38 Zelyonaya Street, Saratov, 410019, Russia*
[3]*Department of Physics and Astronomy, University of Potsdam, Karl-Liebknecht-Strasse 24/25, D-14476 Potsdam-Golm, Germany*

(Received 18 February 2013; revised manuscript received 14 May 2013; published 25 June 2013)

We perform experiments with 72 electronic limit-cycle oscillators, globally coupled via a linear or nonlinear feedback loop. While in the linear case we observe a standard Kuramoto-like synchronization transition, in the nonlinear case, with increase of the coupling strength, we first observe a transition to full synchrony and then a desynchronization transition to a quasiperiodic state. However, in this state the ensemble remains coherent so that the amplitude of the mean field is nonzero, but the frequency of the mean field is larger than frequencies of all oscillators. Next, we analyze effects of common periodic forcing of the linearly or nonlinearly coupled ensemble and demonstrate regimes when the mean field is entrained by the force whereas the oscillators are not.

DOI: 10.1103/PhysRevE.87.062917 PACS number(s): 05.45.Xt, 05.65.+b

## I. INTRODUCTION

An ensemble of many interacting oscillatory units is a popular model, widely used for description of collective dynamics of such various objects as lasers and Josephson junctions, spontaneously beating atrial cells and firing and/or bursting neurons, pedestrians on the footbridges and hand-clapping individuals in a large audience, electrochemical oscillators, metronomes, and many others. Quite often the networks of such elements can be approximately considered as fully connected, with the same strength of interaction within each pair of elements. In this case one speaks of the global or mean-field coupling. Analysis of collective behavior of globally coupled systems is not only important for applications but also poses a number of problems which are highly nontrivial from the standpoint of nonlinear dynamics. Due to these reasons, this topic has remained a focus of interest in the past three decades. Basic theory and further references can be found in Refs. [1–3].

The main effect of global coupling is emergence of a collective mode, or mean field, due to synchronization of some or all elements of the population. The degree of the collective synchrony is reflected in the amplitude of the collective mode; this amplitude is often called the order parameter. Typically, the order parameter increases with the interaction strength, if the latter is larger than a certain threshold value. This effect is well understood within the framework of the Kuramoto-Sakaguchi model [4,5] of sine-coupled phase oscillators, which is analytically solvable in the limit case of infinitely large ensemble. The character of the Kuramoto transition from the incoherent state, where the order parameter is zero, to the partially or fully synchronous state with nonzero mean field depends on the distribution of the natural frequencies within the population; this transition can be either smooth [4,6] or abrupt [7]. The described scenario is not universal, however: Consideration of more complicated oscillators and/or general coupling results in such effects as clustering [8], chaotization of the mean field [9,10], and appearance of robust heteroclinic network attractors [8,11]. Another subject of recent interest is partial synchrony in networks of identical integrate-and-fire units, coupled via the so-called $\alpha$ function, imitating the synaptic delay [10,12]. This model exhibits a collective mode that is not synchronized with individual units, while the synchronous state is unstable. A similar regime was numerically observed for a model of active mechanical oscillators, coupled via an inertial load [13]. Coherent but not synchronous dynamics in ensembles of nonlinearly coupled Stuart-Landau oscillators was demonstrated numerically and analyzed theoretically in the framework of phase approximation in Refs. [14–16]. The latter system demonstrates self-organized quasiperiodic dynamics (SOQ); in this state the frequency of the mean field differs from the frequencies of all oscillators and the dependence of the order parameter on the coupling strength is nonmonotonic. Experimental investigation of such regimes is the primary goal of this paper.

In spite of the high interest in the field, there are relatively few experimental studies of the dynamics of globally coupled systems. Before reviewing these studies, we mention a number of observations of synchronous collective dynamics in systems, where the coupling is assumed to be of the all-to-all type, although it is most likely not homogeneous. This includes observations of the synchronous emission of optical or acoustical pulses by groups of insects [17], rhythmical hand clapping in opera houses [18], glycolytic oscillation in populations of yeast cells [19], etc. A well-known example is pedestrian synchrony on the London Millennium Bridge; the experiments with the pedestrian groups of different sizes demonstrated that collective synchrony is a threshold phenomenon [20], in correspondence with the theoretical results for globally coupled oscillators [4,21]. Next, we mention a brilliant demonstration of collective synchrony in a very simple experiment with metronomes, performed within a framework of student research [22]. Well-controlled experiments on arrays of 64 globally coupled electrochemical oscillators verified most theoretical predictions [23]. In particular, this group provided the first experimental demonstration of the Kuramoto transition for both periodic and chaotic oscillators. Other laboratory experiments have been conducted with Josephson junctions [24], photochemical oscillators [25], vibrating motors on a common support [26], and two groups of metronomes exhibiting chimera states [27].

In this paper we extend our experimental analysis of electronic oscillators, coupled via the common load, communicated in Ref. [28]. Using an experimental setup with 72 units instead of 20, we systematically analyze the ensemble dynamics for the cases of linear and nonlinear coupling. The latter is implemented as follows: The phase shift in the feedback loop depends on the voltage across the common load (mean-field amplitude). We demonstrate that increase of the global coupling first results in the full synchrony and then in its destruction. After synchrony breaking, the system exhibits a quasiperiodic state: Frequency of the mean field is larger than frequencies of all individual oscillators. Next, we investigate the effect of the external forcing of the globally coupled system. Here the main result is a confirmation of the theoretical prediction, made in Ref. [15]. Namely, we show that in case of nonlinear coupling the weak external driving entrains only the mean field but not individual oscillators. Thus, the forced global dynamics remains quasiperiodic.

The paper is organized as follows. In the rest of this section we introduce in more detail the mechanism of appearance of the SOQ dynamics. In Sec. II we present the experimental setup. In Secs. III and IV we describe and discuss the results. Some details of the experiment and mathematical model of the electronic oscillator are presented in the Appendix.

### A. Self-organized quasiperiodic dynamics of globally coupled systems

Consider a system of $N$ all-to-all coupled limit cycle oscillators, where $N$ is large. The dynamics of the collective mode is determined by three factors: (i) dynamics of individual units, (ii) distribution of their parameters, e.g., of frequencies, and (iii) organization of the global coupling. A complete theoretical description of the problem is known only for the case when the oscillators are close to the Hopf bifurcation point and, hence, can be described by the normal form. The equations of the coupled system then read

$$\dot{a}_k = (\mu + i\omega_k)a_k - |a_k|^2 a_k + e^{i\beta}\mathcal{F}\,, \tag{1}$$

where $\mu$ is the Hopf bifurcation parameter (due to the formulated assumption it is positive and small) and $\omega_k$ are natural frequencies of oscillators. Forcing $\mathcal{F}$ depends on the mean field $Z = N^{-1}\sum_k^N a_k$; in the simplest case $\mathcal{F} = \varepsilon Z$, where $\varepsilon$ is the coupling strength. Parameter $\beta$ is an inherent phase shift which describes how the forcing affects individual units.

If $\varepsilon \ll \mu$, the dynamics of Eq. (1) can be described within the framework of phase approximation [2]. For $\mathcal{F} = \varepsilon Z$ this approach yields the paradigmatic Kuramoto-Sakaguchi model [4,5] of sine-coupled oscillators,

$$\dot{\varphi}_k = \omega_k + \varepsilon R \sin(\Theta - \varphi_k + \beta)\,, \quad k = 1,\ldots,N, \tag{2}$$

where $\varphi_k$ are phases of oscillators and $R$ and $\Theta$ are the amplitude and the phase of the complex Kuramoto order parameter (mean field)

$$Re^{i\Theta} = N^{-1}\sum_k e^{i\varphi_k}. \tag{3}$$

[Notice that $R = |Z|/\sqrt{\mu}$ and $\Theta = \arg(Z)$.] For the following it is important that the parameter $\beta$ in Eq. (2) determines the character of the interaction between the oscillators: For $|\beta| < \pi/2$ the coupling is attractive; otherwise, for $\pi/2 < \beta < 3\pi/2$, it is repulsive. The stationary solution of the Kuramoto-Sakaguchi model can be obtained analytically for different frequency distributions [2,7]. Moreover, it admits a complete low-dimensional description in terms of collective variables [16,29].

Generally, the organization of the global coupling can be more complicated than just discussed. So, the mean field can have its own dynamics, described by additional differential equation(s); see, e.g., the models of the array of Josephson junctions [30] and of crowd synchrony on the Millennium Bridge [21]. Physically, it means that the oscillators interact via some medium or common load, which, naturally, can be *nonlinear*. Consider a simple example of medium dynamics:

$$\dot{\mathcal{F}} = -\gamma\mathcal{F} + i\nu\mathcal{F} + i\eta|\mathcal{F}|^2\mathcal{F} + \tilde{\varepsilon}Z. \tag{4}$$

In the linear case $\eta = 0$, the medium is a damped harmonic oscillator (cf. [21,30]); it means that the amplitude of the mean field is multiplied by a constant and its phase is shifted. If the medium is nonlinear, $\eta \neq 0$, the phase shift depends on the mean-field amplitude. As shown below, this feature results in an interesting dynamics.

In the phase approximation, Eqs. (1) and (4) yield extension of the Kuramoto-Sakaguchi model [14]:

$$\dot{\varphi}_k = \omega_k + \varepsilon \sin[\Theta - \varphi_k + \alpha(R,\varepsilon)], \tag{5}$$

where $\varepsilon = \tilde{\varepsilon}/\gamma$ and $\alpha(R,\varepsilon) = \beta + \beta_1\varepsilon^2 R^2$, $\beta_1 = \eta\gamma^{-3}$ [31]. Notice that the phase model of the same form appears if the forcing in Eq. (1) is a nonlinear function of the mean field, $\mathcal{F} = \tilde{\varepsilon}Z + (\eta_1 + i\eta_2)|Z|^2 Z$ [32]. This nonlinear model (5) [33] can exhibit an asynchronous but coherent solution. Indeed, suppose $\omega_k = \omega$ and $|\beta| < \pi/2$. Then, for small $\varepsilon$, the synchronous solution $R = 1$ is stable. However, if the coupling exceeds the critical value, determined by the condition $\pi/2 = \beta + \beta_1\varepsilon_{cr}^2$, synchrony becomes unstable, and the order parameter decreases. On the other hand, if $R$ becomes very small, then $\alpha < \pi/2$ and the coupling again becomes attractive. Thus, the system settles exactly at the border of stability and instability of the fully synchronous solution, so that for $\varepsilon > \varepsilon_{cr}$ we have $\beta + \beta_1\varepsilon^2 R^2 = \pi/2$, or $R = \varepsilon_{cr}/\varepsilon < 1$. In this critical, self-organized state, the mean field has a nonzero amplitude, although the system is not synchronized. Moreover, in this state the frequency of the mean field differs from the oscillator frequency [14]. Since oscillators are not entrained by the mean field, they generally exhibit quasiperiodic dynamics [34]. An analysis of the model (5) was extended to the cases of Lorentzian and uniform frequency distributions [16]. We briefly discuss the latter case, since it is closer to the distribution of oscillator frequencies in our experiment. First, with the increase of $\varepsilon$ the oscillators synchronize. Then, with further increase of $\varepsilon$, they leave the

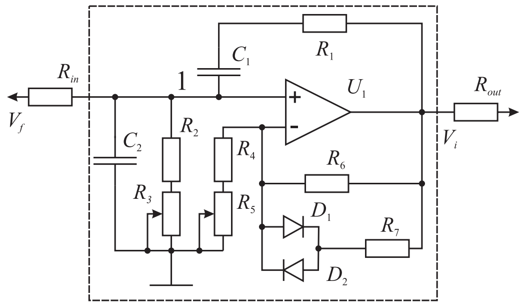


FIG. 1. Wien-bridge oscillator. Here $V_i$ is the output voltage of the $i$th oscillator and $V_f$ is the output voltage of the global feedback loop (cf. Fig. 3).

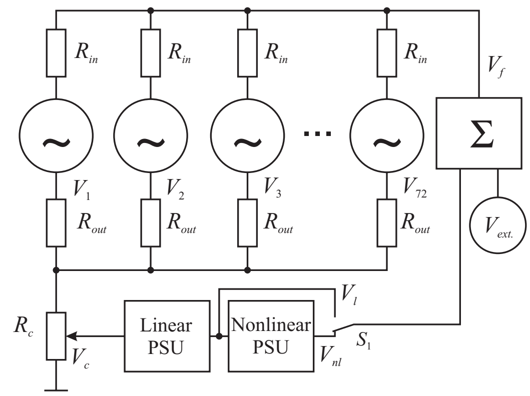


FIG. 3. Scheme of the globally coupled system. Individual generators are shown here by one symbol and a detailed scheme is given in Fig. 1, whereas the schemes of the linear and nonlinear phase-shifting units (PSUs) are given in Fig. 4. With the help of the switch, the nonlinear unit can be excluded from the feedback loop. The strength of the feedback is governed by the potentiometer $R_c$. Common forcing by the external voltage $V_{ext}$ is organized via the summator $\sum$.

synchronous cluster one by one, and finally the SOQ state appears. In this state all oscillators differ in frequency from the mean field; i.e., they all are in a quasiperiodic state.

In summary, nonlinear coupling naturally appears if the oscillators interact via a medium. For cubic nonlinearity and for the oscillators described by the normal form equations, the phase approximation yields the solvable model (5), which exhibits SOQ solutions. Although we cannot perform analytical analysis for general self-sustained oscillators [35], we expect that the emergence of coherent asynchronous regime is mainly determined by the property of the nonlinear coupling, namely by an amplitude-dependent phase shift. Therefore, we expect to observe this state also for systems which go beyond the sine-coupling approximation.

## II. ENSEMBLE OF ELECTRONIC OSCILLATORS

In this section we describe our setup with 72 globally coupled electronic generators. First we present the implementation of an individual unit. Next, we discuss organization of the linear and the nonlinear global coupling and of the common external forcing.

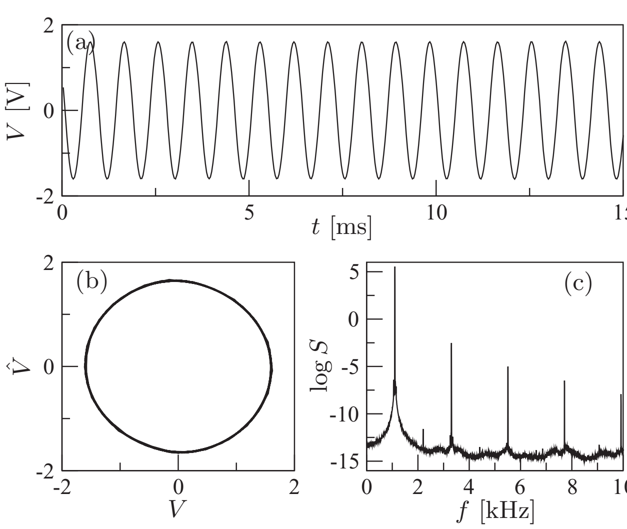


FIG. 2. (a) Output voltage $V$ of an autonomous Wien-bridge oscillator. (b) Limit cycle of the system; here $\hat{V}$ is the Hilbert Transform of $V$. (c) Power spectrum of $V$.

### A. Wien-bridge oscillator

A scheme of an individual generator is given in Fig. 1; it represents a nonlinear amplifier with a positive frequency-dependent feedback via the Wien bridge. The amplifier is implemented by the operational amplifier $U_1$; resistors $R_4$, $R_5$, $R_6$, $R_7$; and diodes $D_1$, $D_2$ [36]. The Wien bridge consists of resistors $R_1$, $R_2$, $R_3$ and capacitors $C_1$, $C_2$. These elements determine the frequency of the oscillation. Fine frequency tuning is performed by the trimmer resistor $R_3$, so that all oscillators in the ensemble have close frequencies $\approx$1.1 kHz. With the help of the trimmer resistor $R_5$ the amplitudes of all uncoupled oscillators were tuned to approximately same value $V \approx 1.5$ V; see Fig. 2. In Appendix we demonstrate that the oscillator is described by an equation of the van der Pol type, which is a paradigmatic model of the nonlinear dynamics [37].

### B. Global coupling and common forcing

Global coupling is organized via the common resistive load $R_c$; see Fig. 3. A fraction of the voltage $V_L$ across this potentiometer is fed back to the individual oscillators via the linear and nonlinear phase-shifting units and resistors $R_{in}$. The input to the feedback loop can be written as $V_c = \varepsilon V_L$, where parameter $\varepsilon$, $0 \leqslant \varepsilon \leqslant 1$, quantifies the strength of the global coupling. It is easy to show that

$$V_c = \varepsilon \frac{\sum_{i=1}^{N} V_i}{N + R_{out}/R_c}, \tag{6}$$

where $V_i$ is the output voltage of the $i$th oscillator. Since $R_{out} \ll N R_c$, we have $V_L \approx N^{-1} \sum V_i = V_{mf}$, where the subscript $mf$ stands for the mean field. Thus, the coupling $V_c \approx \varepsilon V_{mf}$ is of the mean-field type.

The voltage $V_c$ from the common load is fed back to all oscillators via the feedback loop, which includes either linear or both linear and nonlinear phase-shifting units; their schemes are depicted in Fig. 4. The linear subunit is an active all-pass filter which shifts the phase of the signal but keeps

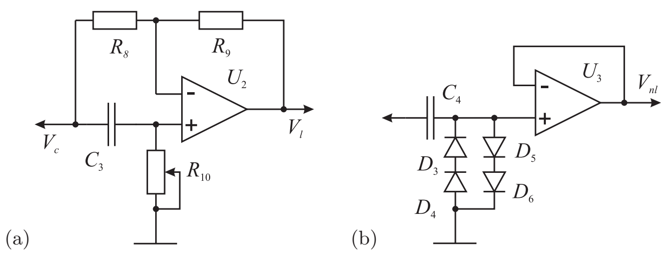


FIG. 4. Linear (a) and nonlinear (b) phase-shifting units.

its amplitude; see Figs. 5(a) and 5(b). The phase induced by the linear PSU is denoted by $\gamma_{lin}$; it can be gradually adjusted by the resistor $R_{10}$ in the range from 0 to $\pi$, as shown in Fig. 5(c). The nonlinear PSU is implemented by a high-pass first-order filter, where nonlinear properties of diodes provide a dependence of the phase shift $\gamma_{nl}$ between input and output on the amplitude of the input [Figs. 5(a) and 5(b)]. Thus, the total phase shift in the feedback loop is $\gamma_{lin} + \gamma_{nl}$, where the first summand serves, along with the coupling coefficient $\varepsilon$, as a control parameter in our experiments, while the second summand depends on the dynamical state of the system. In the experiments with external forcing of the globally coupled ensemble, the sine-wave generated by the NI ELVIS II Instrumentation, Design, and Prototyping Platform was supplied to the feedback loop via a summator.

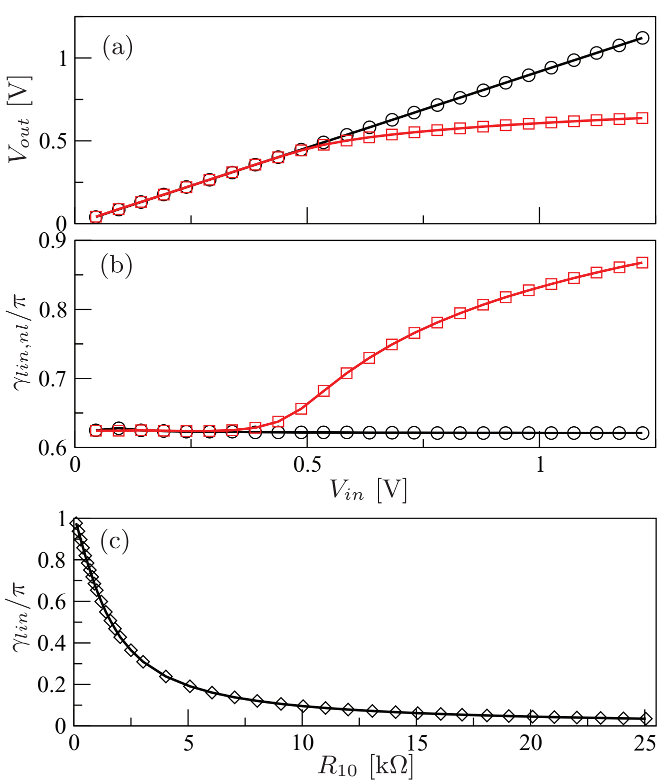


FIG. 5. (Color online) Characteristics of the linear (black circles) and nonlinear (squares, red online) phase-shifting units: (a) output voltage and (b) phase shift $\gamma_{lin,nl} = \phi_{out} - \phi_{in}$ vs the input voltage. (c) Phase shift of the linear unit $\gamma_{lin}$ vs $R_{10}$.

## III. EXPERIMENTAL RESULTS

### A. Acquisition and processing of data

In our experiments we vary parameter $\gamma_{lin}$ of the linear phase-shifting unit, the strength $\varepsilon$ of the global coupling, and the amplitude of the external forcing. For each set of parameters we record output voltages, $V_i$, for all $N = 72$ oscillators and the mean-field voltage, $V_{mf}$, across $R_c$. The sampling frequency is $f_s = 20$ kHz. In each measurement we make five recordings, with $M = 5 \times 10^4$ points per record.

For the presentation of our results we compute the following quantities:

(1) Instantaneous phases $\varphi_i = \arctan(\hat{V}_i / V_i)$, $i = 1, \ldots, 72$, of all oscillators; here $\hat{V}_i$ are Hilbert transforms of $V_i$.

(2) Instantaneous phase $\Theta = \arctan(\hat{V}_{mf} / V_{mf})$ and amplitude $A_{mf} = \sqrt{\hat{V}_{mf}^2 + V_{mf}^2}$ of the mean field, where $\hat{V}_{mf}$ is the Hilbert transform of $V_{mf}$.

(3) Frequencies $f_i$ of all oscillators are obtained from unwrapped phases as $\frac{[\varphi_i(M) - \varphi_i(1)] f_s}{2\pi(M-1)}$ and averaged over five measurements. Mean-field frequency $f_{mf}$ is obtained in a similar way from the unwrapped phase $\Theta$.

(4) The Kuramoto order parameter $R$ is obtained by averaging the quantity $N^{-1} |\sum_{j=1}^{N} e^{i\varphi_j}|$ over $M$ time points and over five measurements.

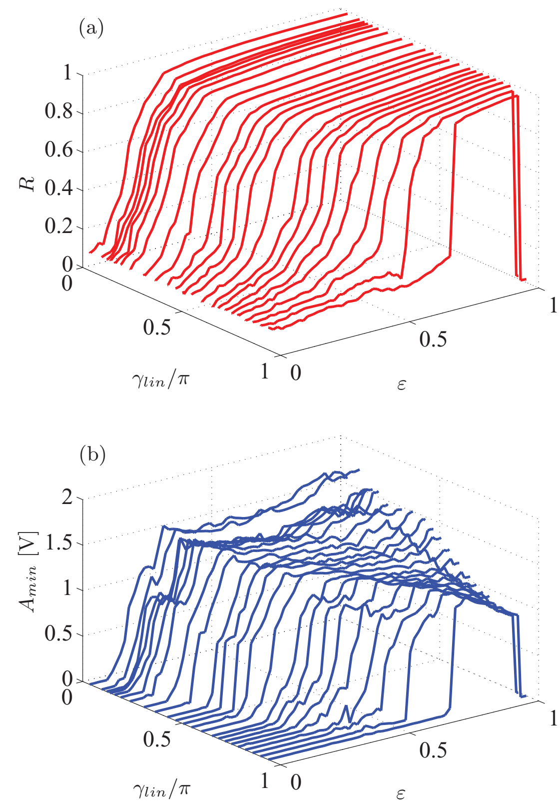


FIG. 6. (Color online) Synchronization transition in ensemble with the linear global feedback loop, for different values of the phase shift $\gamma_{lin}$. In relatively small ensembles, the transitions between coherent and incoherent states can be better traced by the minimal mean-field amplitude $A_{min}$ than by the order parameter $R$; see the text for discussion.

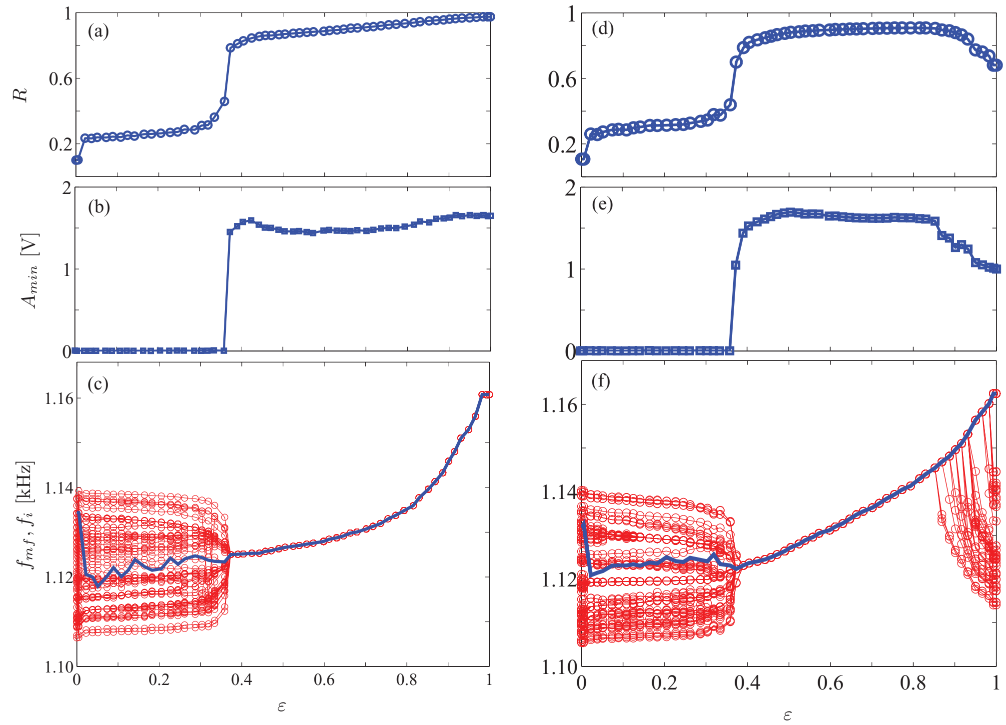


FIG. 7. (Color online) Collective dynamics in ensemble of 72 oscillators with the linear phase-shifting unit in the global feedback loop [panels (a), (b), and (c)] and with both linear and nonlinear PSUs [panels (d), (e), and (f)]; linear phase shift is $\gamma = 0.5\pi$. Order parameter: In the linear case (a) it grows monotonically with $\varepsilon$, but in the nonlinear case (d) the dependence is not monotonic. Panels (b) and (e): Minimal amplitude of the mean field is a measure of the coherence of the ensemble; its deviation from zero reveals the transition to synchrony. Panels (c) and (f): Frequencies of individual oscillators (circles, red online) and of the mean field (solid line, blue online).

(5) The minimal (over time and over all five measurements) value $A_{min}$ of the instantaneous mean-field amplitude $A_{mf}$. As shown in Ref. [28] and as argued below, the deviation of this measure from zero is a good indicator of coherent ensemble dynamics.

We notice that estimates of the instantaneous phases obtained with the help of the Hilbert transform were processed according to Ref. [38]. This processing makes the distribution of the instantaneous phase uniform, as required by the theory, and thus removes some artifacts due to phase reconstruction; see the discussion below.

### B. Collective dynamics of globally coupled ensemble

First we perform the experiments with the linear PSU only. In Fig. 6 we present $R$ and $A_{min}$ in dependence on $\gamma_{lin},\varepsilon$. We see that for the weak coupling, $\varepsilon \lesssim 0.4$, the results qualitatively agree with what we expect for the Kuramoto-Sakaguchi model (2). Indeed, we see that for very small $\gamma_{lin}$ synchronization arises already for very small $\varepsilon$, as reflected by rapid growth of the order parameter $R$. Synchronization transition is delayed for larger $\gamma_{lin}$, as is the case of the model (2), and for $\gamma_{lin} \gtrsim \pi/2$ the ensemble remain asynchronous. We emphasize that this comparison is qualitative since we cannot directly associate $\gamma_{lin}$ and parameter $\alpha$ in Eq. (2), e.g., because the forcing of the oscillators is represented by a combination of the mean field and its derivative; see Eq. (A2). For the strong coupling, $\varepsilon \gtrsim 0.5$, the dynamics is different from that of the phase model; in particular, for $\gamma_{lin} \approx 0.95\pi$ the dependence of $R$ on $\varepsilon$ becomes nonmonotonic and for $\varepsilon \approx 1$ the synchrony breaks up.

Figures 7(a)–7(c) and 8(a)–8(c) show in detail the dynamics of coupled oscillators for two particular settings of the linear PSU, i.e., for $\gamma_{lin} \approx 0.5\pi$ and $\gamma \approx 0.65\pi$. In Figs. 7(d)–7(f) and 8(d)–8(f) we show for comparison the main results for the case of our interest, namely when the nonlinear PSU in the global feedback loop is switched on. As expected, in the linear case we observe a monotonic growth of the order parameter $R$ with the coupling strength $\varepsilon$. Due to the finite size of the ensemble, $R$ is not small in the asynchronous state; the transition to synchrony is much better characterized by the minimal mean-field amplitude $A_{min}$ [28]; see also discussion of Fig. 9 below. One can see that $A_{min}$ is practically zero when frequencies of oscillators differ and it starts to grow when some oscillators synchronize. Generally, we can understand $A_{min}$ as a measure of coherence of the ensemble. Indeed, if the finite-size ensemble is in a coherent state (synchronous or partially synchronous), the mean field looks like a periodic process, corrupted by some noise [39], and its minimal amplitude essentially deviates from zero. Otherwise, if the ensemble is in an asynchronous state, the mean field fluctuates and looks like filtered noise; the amplitude then can be very small. We emphasize that the main source of the mean-field fluctuations is the small ensemble size $N = 72$. The thermal noise in the setup is rather small: The variations of the oscillators' frequencies for repeated measurements are less than 0.1%.

Now we discuss the case when the nonlinear PSU is switched on. The transitions for $\gamma_{lin} \approx 0.5\pi$ and $\gamma_{lin} \approx 0.65\pi$ are shown in Figs. 7(d)–7(f) and 8(d)–8(f). We see that

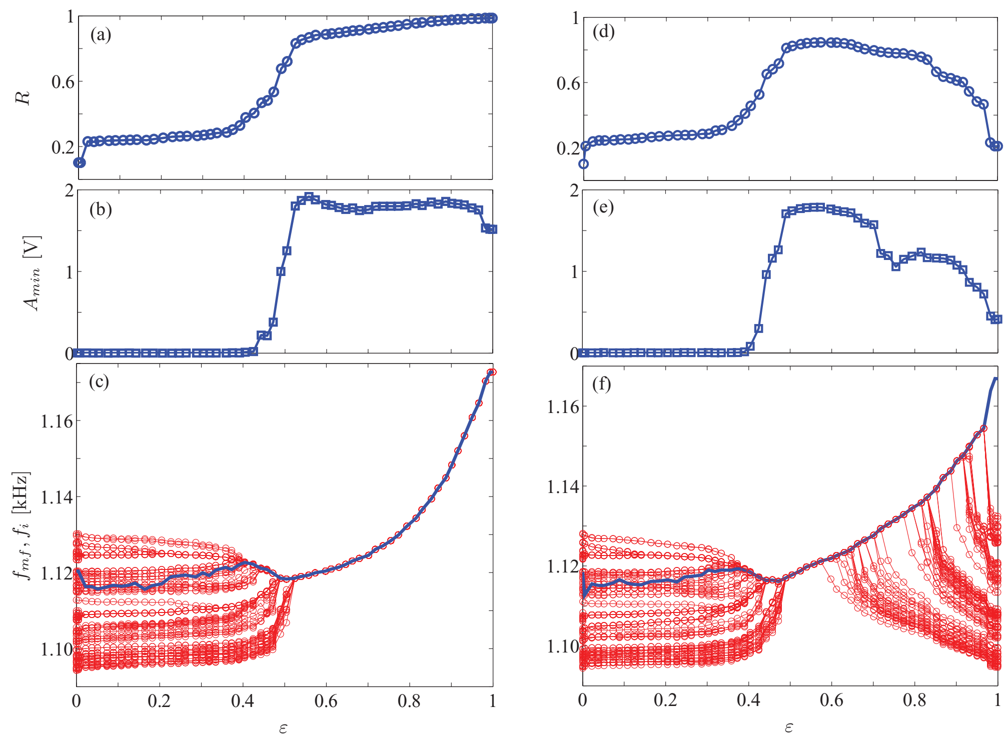


FIG. 8. (Color online) Same as in Fig. 7 but for $\gamma_{lin} = 0.65\pi$.

the oscillators synchronize for the coupling $\varepsilon \approx 0.35$ and $\varepsilon \approx 0.5$, respectively, and then synchrony becomes unstable. The slow oscillators leave the synchronous group and the order parameter decreases. For $\gamma_{lin} \approx 0.65\pi$ and for sufficiently large coupling all oscillators are not entrained by the mean field. However, the mean field has a nonzero amplitude; i.e., the SOQ state emerges. The picture quantitatively coincides with the theoretical and numerical result for phase oscillators in Eq. (5) with uniform frequency distribution [16].

In order to get more insight into the collective dynamics, we illustrate in detail two states, for $\gamma_{lin} = 0.65\pi$ and coupling $\varepsilon$=0.0048 and $\varepsilon$=1 (see Fig. 9). The value of the time-averaged order parameter is nearly the same for both cases, $R \approx 0.2$; however, as can be seen from the dynamics of the mean field, these states are, respectively, noncoherent and coherent.

### C. Phase dynamics from data

Here we check whether the dynamics of our experimental setup is consistent with the mechanism of the SOQ described in Ref. [14] within the framework of Eq. (5). We recall that this mechanism implies that the system settles at the border between synchrony and asynchrony, so that the synchronous solution becomes neutrally stable. Neutral stability means that the derivative of the coupling function computed for the phase difference $\Theta - \varphi_i$ in the synchronous state is zero. To check this, we pick up two data sets, obtained for the phase shift $\gamma_{lin} = 0.65\pi$ and close values of the coupling strength. For the first value, $\varepsilon = 0.573$, the system is synchronous, and all oscillator frequencies are equal. If coupling is increased to $\varepsilon = 0.598$, the system undergoes a desynchronization transition when one oscillator (let its index be $k$) leaves the synchronous group. Notice that $N-1$ oscillators which remain in the group have same frequencies, though different phases. By neglecting the contribution of the $k$th oscillator to the mean field $V_{mf}$, we can consider this oscillator as driven by $V_{mf}$ and search for the phase model in the form

$$\dot{\varphi}_k = \omega + H(\Theta - \varphi_k), \tag{7}$$

where $H(x) = H(x+2\pi)$, cf. [40]. In order to reconstruct Eq. (7) we estimate the instantaneous frequency $\dot{\varphi}$ with the help of the Savitsky-Golay filter of order 4. Next, we fit the dependence $\dot{\varphi}_k(t)$ on $\Theta - \varphi_k$ by a Fourier series of the order 10; the results are shown in Fig. 10.We emphasize that model reconstruction is not possible for $\varepsilon = 0.573$, because here the phase difference attains only one value $\Theta - \varphi_k \approx 1.2$.

Before interpreting the reconstructed model, we emphasize that prior to numerical derivation and to Fourier fitting both phases are transformed according to Ref. [38]. The idea behind this transformation is as follows: Suppose we estimate the oscillator's phase from a scalar signal with the help of the Hilbert transform or any other embedding. Let us denote this estimate (protophase) as $\psi$. For an autonomous system we generally have $\dot{\psi} = \omega + g(\psi)$, while the true phase obeys $\dot{\varphi} = \omega$ [2]. Function $g(\psi)$ depends on the observable and the embedding; it reflects the nonuniformity of motion along the limit cycle. In the theory, $g(\theta)$ is always eliminated by a simple transformation; see, e.g., Ref. [3]. If the oscillator interacts with others, the true phase obeys Eq. (7), while for the protophase we have $\dot{\psi} = \omega + g(\psi) + \hat{H}$. If the interaction is small (which is the most interesting case), then the nonuniformity of phase growth due to the coupling function $\hat{H}$ is smaller than that due to the function $g$, which essentially complicates recovery of interaction. Next, $\psi$ and $g$ depend on the embedding and observables, while $\varphi$ and $H$ are unique; the

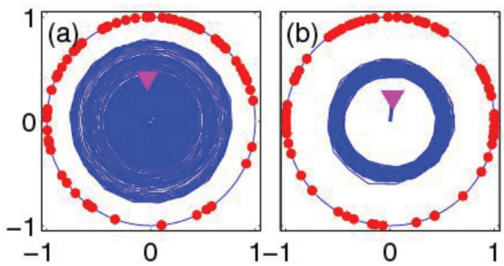


FIG. 9. (Color online) Collective dynamics of the electronic ensemble for $\gamma_{lin} = 0.65\pi$ and $\varepsilon = 0.0048$ (a) and $\varepsilon = 1$ (b). Here red (gray) circles show the snapshot of oscillator phases on the unit circle. We see that in both cases the phases are scattered, though their distribution is nonuniform. Magenta (gray) triangles show the instantaneous complex order parameter. Blue (gray) solid lines show the phase portrait of the mean field in $V,\hat{V}$ coordinates, where $\hat{V}$ is the Hilbert transform of the mean field $V$, measured in volts. (Notice that the amplitude of the mean field is directly related to the nonuniformity of phase distribution: zero mean field corresponds to the uniform distribution.) These plots clearly demonstrate the difference in the dynamics of the two states: In panel (a) the nonuniformity of the phase distribution changes with time and, therefore, the amplitude of the mean field fluctuates and sometimes drops practically to zero, as we would expect for a noisy process; these fluctuations are due to the relatively small ensemble size. This picture is typical for asynchronous, noncoherent dynamics. In panel (b) the mean-field dynamics resembles that of a noisy limit cycle; the fluctuation of the mean-field amplitude is relatively small. Though all oscillators here have different frequencies, they exhibit coherent collective motion.

transformation [38] ensures invariant model reconstruction. Practically, it is performed according to

$$\varphi = \psi + 2\sum_{n=1}^{n_F} \mathrm{Im}\left[\frac{S_n}{n}(e^{in\psi} - 1)\right],$$

where $S_n = n^{-1}\sum_{j=1}^{N} e^{-in\psi(t_j)}$ are the coefficients of the Fourier expansion of the probability distribution density of $\psi$, computed from its time series $\psi(t_j)$, where $j = 1,\ldots,N$. The optimal number $n_F$ of the Fourier modes is determined according to Ref. [41]; MATLAB code for the transformation is available upon request from the authors. This *invertible* transformation eliminates the component of the instantaneous frequency which depends on $\psi$ only, so that on average the transformed phase grows uniformly in time. For our data, this transformation is crucial for a successful model reconstruction: Without the transformation the plotted dependence $\dot{\phi}_k$ vs $\Theta - \phi_k$ exhibits no structure. It means that deviation from the uniform phase growth due to the external forcing (the issue of our interest) is small if compared to the systematic $\phi_k$-dependent variation of the instantaneous frequency, which is an artifact of the phase plane reconstruction.

In Fig. 10(a) we see that frequencies of the chosen oscillator and of the mean field are indeed different: The $\Theta$ vs $\varphi_k$ plot exhibits a typical picture of nearly synchronous behavior with phase slips. Due to these slips, the trajectory fills the square and makes the reconstruction possible. In Fig. 10(b) we see that the coupling function attains the maximum exactly at the phase shift $\Theta - \phi_k$ corresponding to the synchronous solution, which indicates the neutral stability of the observed dynamical states and therefore confirms consistency of interpretation of the dynamics after the synchrony breaking in terms of SOQ.

### D. Globally coupled ensemble under periodic forcing

In this section we present the results of experiments where linearly or nonlinearly coupled ensemble was forced by a common periodic signal. This problem was theoretically addressed in Refs. [42,43]; the case of the nonlinearly coupled ensemble in the SOQ state was treated in Ref. [15]. Investigation of the common forcing of large ensembles is relevant, e.g., for neuroscience, where this model can be used for description of rhythms of a large neuronal population, influenced by the rhythms from other brain regions. In the first approximation the ensemble exhibiting a collective mode can be considered as a macroscopic oscillator, and therefore it is natural to expect that

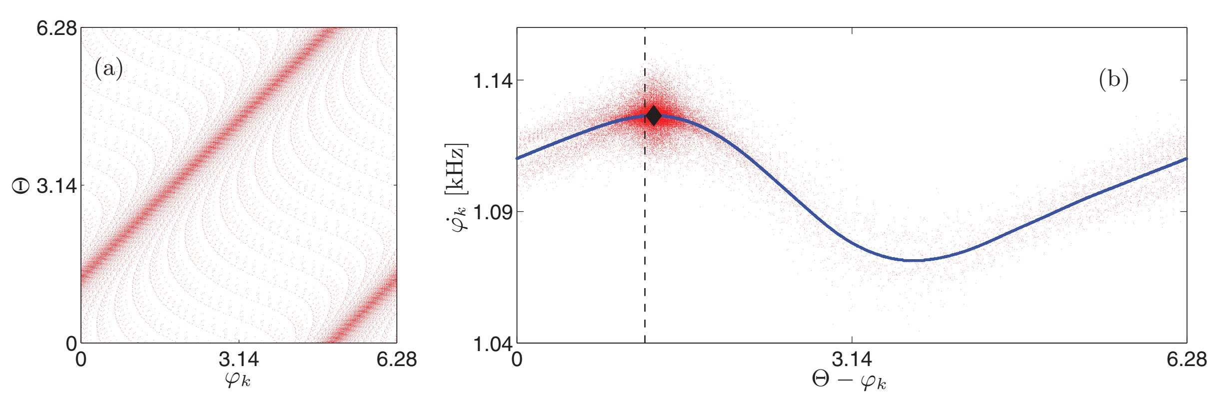


FIG. 10. (Color online) Phase model of the system, reconstructed from data, for $\varepsilon = 0.598$ and $\gamma_{lin} = 0.65\pi$. Here the ensemble is close to the synchrony breaking point: $N - 1$ oscillators form the synchronous group and one oscillator, labeled by index $k$, is asynchronous with respect to the majority, as can be seen from the plot of $\varphi_k$ vs the phase $\Theta$ of the mean field (a). Panel (b) shows the recovered coupling function $\dot{\varphi}_k = H(\Theta - \varphi_k)$; here red (gray) dots show the data points while the blue (gray) line is obtained via Fourier fit; it can be interpreted as the reconstructed coupling function $H$ [see Eq. (7)]. The maximum of the coupling function is marked by the black diamond; the dashed line shows the value of $\Theta - \varphi_k$ for slightly smaller $\varepsilon = 0.573$, when complete synchrony is observed. Zero derivative of the coupling function at the synchronous solution indicates neutral stability of the latter, which is a characteristic feature of the self-organized quasiperiodic dynamics.

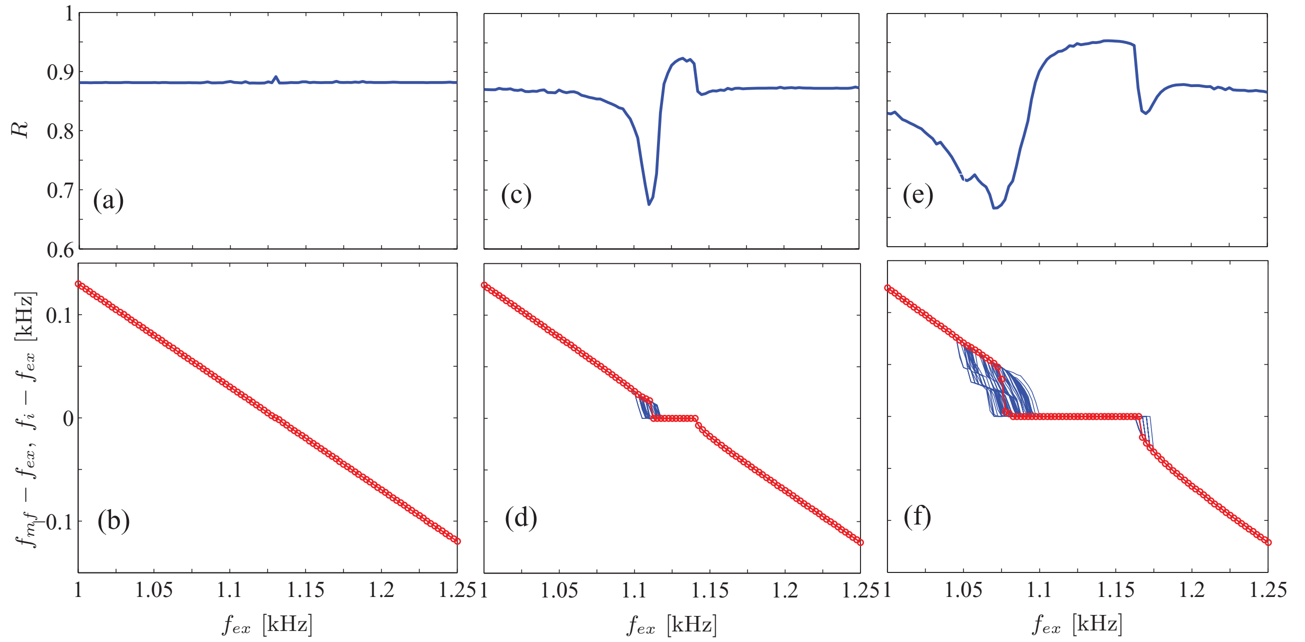


FIG. 11. (Color online) Results of harmonic forcing of the linearly coupled ensemble, for three different amplitudes of the force: 0.08 (a), (b); 0.5 (c), (d); and 1.5 (e), (f). Here $f_{ex}$ is the frequency of the common external forcing. $f_{mf} - f_{ex}$ is shown with red (gray) dots, and $f_i - f_{ex}$ is shown by blue (gray) lines; $\gamma_{lin} = 0.65\pi$, $\varepsilon = 0.57$.

it can be entrained by an external forcing. However, if we go beyond this simplistic description and consider the dynamics on the level of individual units, we can expect different effects. So, in the case of the harmonically forced Kuramoto model one observes formation of synchronous subpopulations of oscillators with different frequencies [42]. For the nonlinearly coupled ensemble in the SOQ state, the theory for identical oscillators [15] predicts that external force can lock the mean field without entraining individual oscillators. Here we verify this prediction.

Results on forcing the linearly coupled ensemble are presented in Fig. 11 (cf. [44]), to be compared with the results for nonlinear coupling, given in Fig. 12. First, we see that in both cases the mean field is entrained by the external force, if the amplitude of the forcing exceeds a critical value. Such behavior is typical for noisy and chaotic oscillators. Since the mean field of a finite-size ensemble is not exactly periodic but fluctuates, it is natural that the response of the ensemble to an external forcing is similar to the response of a macroscopic noisy oscillator. Next, we see that in the linear case the entrainment of the mean field is always accompanied by the entrainment of at least some subpopulation of oscillators. In contrast, in the case of the ensemble in the SOQ state, we observe regimes where the mean field is locked to the external force but the oscillators are not. Thus, the system remains in the SOQ state. For stronger coupling we have

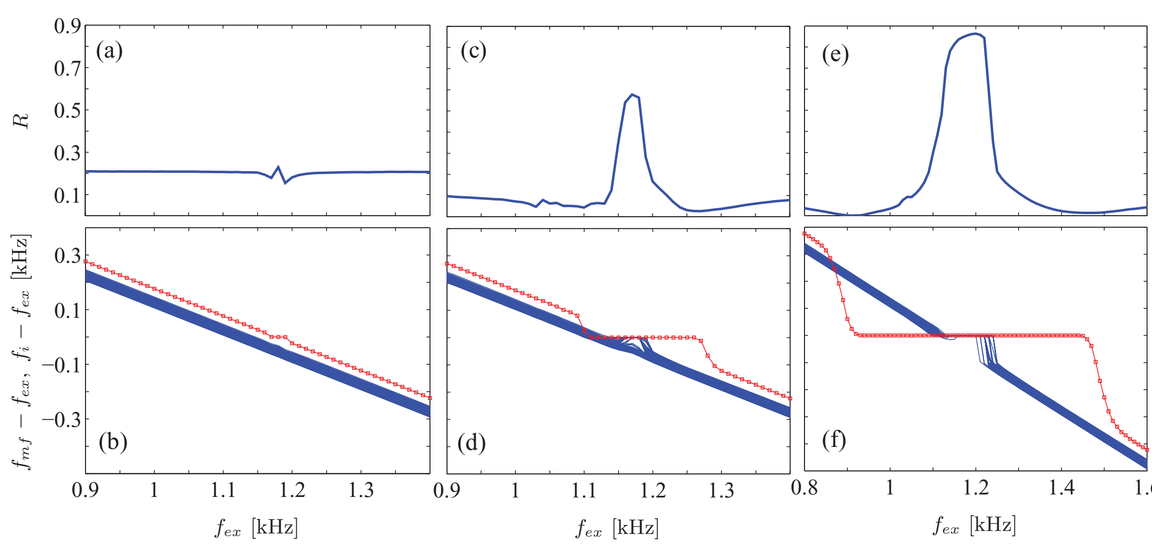


FIG. 12. (Color online) The same as in Fig. 11, but for the nonlinearly coupled ensemble. Feedback parameters are $\gamma_{lin} = 0.65\pi$, $\varepsilon = 0.98$.

both SOQ and fully synchronous states. It means that for some (relatively narrow) range of external frequencies, the force destroys the quasiperiodic dynamics and imposes full synchrony; this is accompanied by an essential increase (up to three times) of the order parameter. In the linear case, the variation of the order parameter with $f_{ex}$ is not so strong and can be easily understood as follows. When $f_{ex}$ is close to the mean-field frequency (i.e., it is in the middle of the synchronization plateau), the forcing facilitates synchrony. However, since the oscillators are already synchronized, the increase of the order parameter is not large. When $f_{ex}$ is outside of the synchronization region but close to it, then some part of the population synchronizes with the forcing, while the rest remains in the synchronous cluster; as a result, the order parameter decreases.

## IV. DISCUSSION

We have performed experiments with an ensemble of 72 globally coupled van der Pol–like electronic oscillators, treating the cases of linear and nonlinear coupling. The nonlinear coupling was implemented via a circuit with an amplitude-dependent phase shift. We have observed synchronous ensemble dynamics, with all elements of the ensemble oscillating with a common frequency. Next, we have shown that in case of nonlinear feedback, increase of coupling results in synchrony breaking, but the ensemble remains in a coherent state. In this state, all oscillators have different frequencies, but, contrary to the simple case of asynchronous dynamics, their phases are distributed nonuniformly and therefore the oscillators produce a nonzero, coherent mean field whose frequency is larger than all oscillator frequencies. Thus, oscillators are not frequency locked to the mean field and therefore exhibit quasiperiodic behavior. With these observations we extended the theoretical predictions for sine-coupled oscillators [14,15] to a different class of systems, namely to van der Pol oscillators. We emphasize that the van der Pol model not only played a central role in the development of nonlinear science [45], but also describes, together with the equivalent Rayleigh model [46], a variety of natural phenomena; see, e.g., Ref. [37] and references therein.

Global nonlinear coupling is a less explored topic. However, such coupling naturally arises if oscillators interact via a medium with nonlinear properties. Another option is coupling via a transmission line with amplitude-dependent velocity of signal propagation; such setup can be described by an amplitude-dependent time delay in the feedback loop, what is roughly equivalent to amplitude-dependent phase shift. Our results shed lights on the importance of the latter property of the global coupling. We believe that the mechanism leading to synchrony breaking and emergence of SOQ dynamics due to amplitude-dependent phase shift in the feedback loop is quite general. Indeed, previously this mechanism was demonstrated theoretically for normal form oscillators and numerically for nonlinearly coupled Josephson junctions [14], which represent a different class of systems (rotators). Here we have shown this mechanism for van der Pol–like systems. (Notice that our system cannot be described by the Kuramoto model, because the phase coupling function is not a sine; see Fig. 10). We conclude that common properties of collective dynamics of these different systems indicate a decisive role of the nonlinear coupling. Since the Kuramoto and the van der Pol equations represent only an approximate description of real dynamics, we are convinced that it was important to demonstrate the robustness of the effect in a physical experiment.

Furthermore, we conducted experiments with periodic forcing of the globally coupled ensemble and compared the results with the theory developed in Ref. [16]; we have demonstrated that external forcing can entrain the mean field, without locking individual units. We believe that our results are relevant for investigation of other oscillator populations with amplitude-dependent phase shift or time delay in the global feedback loop. As a possible direction for future experiments we mention investigation of different forms of nonlinear coupling and of different scenarios of transitions from synchrony to asynchronous, though coherent states.

## ACKNOWLEDGMENTS

We gratefully acknowledge helpful discussion with M. Zaks and A. Pikovsky. V.P. acknowledges financial support from RFFI Grant No. 12-02-00377.

## APPENDIX: EQUATION OF THE WIEN-BRIDGE OSCILLATOR

The experimentally obtained input-output characteristic of the operational amplifier along with its analytical approximation is shown in Fig. 13(a). For the range of input voltages $u$ that is of interest for us, the characteristic can be well approximated by the fifth-order polynomial

$$V_a = f(u) = a_1 u - a_3 u^3 + a_5 u^5, \tag{A1}$$

where $a_1 = 3.1557$, $a_3 = 0.8072$, and $a_5 = 0.95282$; the approximation is illustrated by Fig. 13(b).

Now we derive the equation of the oscillator, driven by external voltage $V_f$. Denoting the input and output voltages of the operational amplifier as $u$ and $V$, respectively, and the input-output characteristics of the amplifier as $V = f(u)$ [see Eq. (A1)], we write the Kirchhoff laws for balance of currents

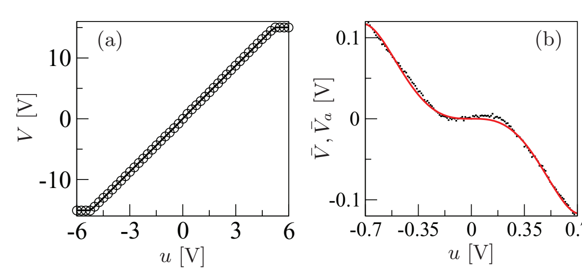


FIG. 13. (Color online) (a) Experimentally obtained input-output characteristics of the operational amplifier. (b) Practically, the generator operates in the regime where input voltages are approximately in the interval from $-0.7$ to 0.7 V, which corresponds to the output voltages in the range $\pm 2$ V. This region can be well approximated by the fifth-order polynomial; see Eq. (A1). Here the characteristic $V(u)$ and its approximation $V_a(u)$ are shown by black symbols and the red (gray) line, respectively. For better visibility the linear growth is subtracted: here $\bar{V} = V - a_1 u$, $\bar{V}_a = V_a - a_1 u$.

and voltages at point 1 in Fig. 1:

$$I = C_2\dot{u} + \frac{u}{R_2+R_3} + \frac{u-V_f}{R_{in}},$$
$$f(u) = u + IR_1 + \frac{1}{C_1}\int I dt,$$

where $I$ is the current through the $R_1C_1$ grid. Using $C_1 = C_2$, excluding $I$ and differentiating with respect to time, we obtain with the help of Eq. (A1) the equation of the van der Pol type:

$$\ddot{u} - \mu(1-\alpha u^2+\beta u^4)\dot{u} + \Omega^2 u = \nu\dot{V}_f + \nu\omega V_f. \quad \text{(A2)}$$

The parameters here are $\omega = (R_1C_1)^{-1}$, $\nu = (R_{in}C_1)^{-1}$, $\Omega^2 = \frac{\omega}{(R_2+R_3)C_1} + \omega\nu$ ,$\mu = \omega\eta$, $\alpha = 3a_3\eta^{-1}$, and $\beta = 5a_5\eta^{-1}$, where

$$\eta = a_1 - 2 - \frac{R_1}{R_2+R_3} - \frac{R_1}{R_{in}}.$$

For the given components, the latter parameter is $0.10 \lesssim \eta \lesssim 0.29$, in dependence on the resistance of the trimmer potentiometer $R_3$. For positive values of $\eta$ and, respectively, positive $\mu$, Eq. (A2) exhibits a limit-cycle solution.


[1] A. T. Winfree, *The Geometry of Biological Time* (Springer, Berlin, 1980).

[2] Y. Kuramoto, *Chemical Oscillations, Waves, and Turbulence* (Springer, Berlin, 1984).

[3] A. Pikovsky, M. Rosenblum, and J. Kurths, *Synchronization: A Universal Concept in Nonlinear Sciences.* (Cambridge University Press, Cambridge, 2001); D. Golomb, D. Hansel, and G. Mato, in *Neuro-informatics and Neural Modeling*, Handbook of Biological Physics Vol. 4, edited by F. Moss and S. Gielen (Elsevier, Amsterdam, 2001), pp. 887–968; S. H. Strogatz, Phys. D (Amsterdam, Neth.) **143**, 1 (2000); *Sync: The Emerging Science of Spontaneous Order* (Hyperion, New York, 2003); E. Ott, *Chaos in Dynamical Systems*, 2nd ed. (Cambridge University Press, Cambridge, 2002); S. C. Manrubia, A. S. Mikhailov, and D. H. Zanette, *Emergence of Dynamical Order: Synchronization Phenomena in Complex Systems*, Lecture Notes in Complex Systems Vol. 2 (World Scientific, Singapore, 2004); J. A. Acebron, L. L. Bonilla, C. J. P. Vicente, F. Ritort, and R. Spigler, Rev. Mod. Phys. **77**, 137 (2005); M. Breakspear, S. Heitmann, and A. Daffertshofer, Front. Human Neurosci. **4**, 190 (2010).

[4] Y. Kuramoto, in *International Symposium on Mathematical Problems in Theoretical Physics*, edited by H. Araki, Lecture Notes in Physics Vol. 39 (Springer, New York, 1975), p. 420.

[5] H. Sakaguchi and Y. Kuramoto, Prog. Theor. Phys. **76**, 576 (1986).

[6] H. Daido, Phys. Rev. Lett. **73**, 760 (1994).

[7] D. Pazó, Phys. Rev. E **72**, 046211 (2005).

[8] K. Okuda, Phys. D (Amsterdam, Neth.) **63**, 424 (1993); H. Kori and Y. Kuramoto, Phys. Rev. E **63**, 046214 (2001); Z. Liu, Y.-C. Lai, and F. C. Hoppensteadt, *ibid.* **63**, 055201 (2001); Y. Maistrenko, O. Popovych, O. Burylko, and P. A. Tass, Phys. Rev. Lett. **93**, 084102 (2004).

[9] P. C. Matthews and S. H. Strogatz, Phys. Rev. Lett. **65**, 1701 (1990); V. Hakim and W. J. Rappel, Phys. Rev. A **46**, R7347 (1992); N. Nakagawa and Y. Kuramoto, Prog. Theor. Phys. **89**, 313 (1993); Phys. D (Amsterdam, Neth.) **75**, 74 (1994).

[10] S. Olmi, A. Politi, and A. Torcini, Europhys. Lett. **92**, 60007 (2010).

[11] D. Hansel, G. Mato, and C. Meunier, Phys. Rev. E **48**, 3470 (1993); H. Kori, *ibid.* **68**, 021919 (2003); P. Ashwin, G. Orosz, and J. Borresen, in *Nonlinear Dynamics and Chaos: Advances and Perspectives (Understanding Complex Systems)*, edited by M. Thiel *et al.* (Springer, Berlin, 2010), pp. 31–50.

[12] C. van Vreeswijk, Phys. Rev. E **54**, 5522 (1996); P. Mohanty and A. Politi, J. Phys. A: Math. Gen. **39**, L415 (2006).

[13] A. Vilfan and T. Duke, Phys. Rev. Lett. **91**, 114101 (2003).

[14] M. Rosenblum and A. Pikovsky, Phys. Rev. Lett. **98**, 064101 (2007); A. Pikovsky and M. Rosenblum, Phys. D (Amsterdam, Neth.) **238**, 27 (2009).

[15] Y. Baibolatov, M. Rosenblum, Z. Z. Zhanabaev, M. Kyzgarina, and A. Pikovsky, Phys. Rev. E **80**, 046211 (2009).

[16] Y. Baibolatov, M. Rosenblum, Z. Z. Zhanabaev, and A. Pikovsky, Phys. Rev. E **82**, 016212 (2010); A. Pikovsky and M. Rosenblum, Phys. D (Amsterdam, Neth.) **240**, 872 (2011).

[17] J. Buck and E. Buck, Science **159**, 1319 (1968).

[18] Z. Néda, E. Ravasz, Y. Brechet, T. Vicsek, and A.-L. Barabási, Nature (London) **403**, 849 (2000).

[19] P. Richard, B. M. Bakker, B. Teusink, K. V. Dam, and H. V. Westerhoff, Eur. J. Biochem. **235**, 238 (1996); S. Danø, P. G. Sørensen, and F. Hynne, Nature (London) **402**, 320 (1999).

[20] P. Dallard, T. Fitzpatrick, A. Flint, A. Low, R. R. Smith, M. Willford, and M. Roche, J. Bridge Eng. **6**, 412 (2001).

[21] S. H. Strogatz, D. M. Abrams, A. McRobie, B. Eckhardt, and E. Ott, Nature (London) **438**, 43 (2005).

[22] See http://go.owu.edu/~physics/StudentResearch/2005/BryanDaniels/index.html for description and video of the experiment.

[23] W. Wang, I. Z. Kiss, and J. L. Hudson, CHAOS **10**, 248 (2000); Phys. Rev. Lett. **86**, 4954 (2001); I. Z. Kiss, W. Wang, and J. L. Hudson, CHAOS **12**, 252 (2002); I. Kiss, Y. Zhai, and J. Hudson, Science **296**, 1676 (2002).

[24] P. Barbara, A. B. Cawthorne, S. V. Shitov, and C. J. Lobb, Phys. Rev. Lett. **82**, 1963 (1999); G. Filatrella, N. F. Pedersen, and K. Wiesenfeld, Phys. Rev. E **61**, 2513 (2000).

[25] A. F. Taylor, P. Kapetanopoulos, B. J. Whitaker, R. Toth, L. Bull, and M. R. Tinsley, Phys. Rev. Lett. **100**, 214101 (2008).

[26] D. Mertens and R. Weaver, Complexity **16**, 4553 (2011).

[27] E. A. Martens, S. Thutupalli, A. Fourrière, and O. Hallatschek, PNAS Early Edition (2013), doi: 10.1073/pnas.1302880110.

[28] A. A. Temirbayev, Z. Z. Zhanabaev, S. B. Tarasov, V. I. Ponomarenko, and M. Rosenblum, Phys. Rev. E **85**, 015204 (2012).

[29] S. Watanabe and S. H. Strogatz, Phys. Rev. Lett. **70**, 2391 (1993); Phys. D (Amsterdam, Neth.) **74**, 197 (1994); E. Ott and T. M. Antonsen, CHAOS **18**, 037113 (2008); **19**, 023117 (2009).

[30] K. Wiesenfeld and J. W. Swift, Phys. Rev. E **51**, 1020 (1995).

[31] Notice that the model $\dot{\varphi}_k = \omega_k + A(R,\varepsilon)sin(\Theta-\varphi_k)$ with an amplitude function $A$ was considered in Ref. [47].

[32] M. Rosenblum and A. Pikovsky (unpublished).

[33] The model can be denoted as nonlinear due to the following reasoning: Consider for simplicity identical oscillators, $\omega_k = \omega$. Stability of the synchronous solution $\varphi_k = \varphi = \Theta$, $R = 1$ is quantified by the eigenvalue $\lambda = -\varepsilon \cos(\alpha(1,\varepsilon))$. If $\alpha = \text{const}$ (the Kuramoto-Sakaguchi case) and $|\alpha| < \pi/2$, the coupling is attractive for all $\varepsilon$ and the stability of the synchronous state grows linearly with $\varepsilon$. In a general case, $\lambda$ can change its sign with the variation of $\varepsilon$, so that the attractive coupling becomes repulsive, and vice versa; i.e., the stability nonlinearly depends on $\varepsilon$.

[34] The mean-field frequency is larger than those of oscillators if $\alpha$ crosses the upper border $\pi/2$. In the opposite case, when $\alpha$ becomes smaller than $-\pi/2$, the mean field is slower than oscillators.

[35] Generally, a phase approximation description is given by the Daido model [48] with an arbitrary coupling function of the phase difference, $\Theta - \varphi_k$; the dynamics of this model can essentially differ from that of the Kuramoto-Sakaguchi model.

[36] The specifications of the components used are as follows. Elements of the Wien-bridge oscillator are $R_1 = 2.2\,k\Omega$, $R_2 = 2.15\,k\Omega$, $R_3 = 500\,\Omega$ (trimmer potentiometer, it was used to tune the oscillators frequency), $C_{1,2} = 51\,nF$, $R_4 = 2.2\,k\Omega$, $R_5 = 5\,k\Omega$ (trimmer potentiometer, it was used to tune the amplitudes of oscillators), $R_6 = 10\,k\Omega$, $R_7 = 40.2\,k\Omega$. Elements of the feedback loop are $R_{in} = 62\,k\Omega$, $R_{out} = 1\,k\Omega$, $R_c = 10\,k\Omega$, $R_8 = R_9 = 6.2\,k\Omega$, $R_{10} = 50\,k\Omega$ (trimmer resistor, it was used to change the linear phase shift), $C_{3,4} = 100\,nF$. The operational amplifiers and diodes are of the type AD822 and LL4148, respectively.

[37] I. I. Blekhman, *Synchronization in Science and Technology* (Nauka, Moscow, 1981) (in Russian; English translation: 1988, ASME Press, New York); P. S. Landa, *Nonlinear Oscillations and Waves in Dynamical Systems* (Kluwer Academic Publishers, Dordrecht, 1996); S. Peleš and K. Wiesenfeld, Phys. Rev. E **68**, 026220 (2003).

[38] B. Kralemann, L. Cimponeriu, M. Rosenblum, A. Pikovsky, and R. Mrowka, Phys. Rev. E **76**, 055201 (2007); **77**, 066205 (2008).

[39] Generally, the mean field can be also chaotic.

[40] R. F. Galán, G. B. Ermentrout, and N. N. Urban, Phys. Rev. Lett. **94**, 158101 (2005); I. Z. Kiss, Y. Zhai, and J. L. Hudson, *ibid.* **94**, 248301 (2005); J. Miyazaki and S. Kinoshita, *ibid.* **96**, 194101 (2006).

[41] C. Tenreiro, J. Nonparametric Stat. **23**, 533 (2011).

[42] H. Sakaguchi, Prog. Theor. Phys. **79**, 39 (1988).

[43] L. M. Childs and S. H. Strogatz, CHAOS **18**, 043128 (2008); K. Okuda and Y. Kuramoto, Prog. Theor. Phys. **86**, 1159 (1991).

[44] I. Z. Kiss, Y. Zhai, and J. L. Hudson, Phys. Rev. E **77**, 046204 (2008).

[45] S. H. Strogatz, *Nonlinear Dynamics and Chaos: With Applications to Physics, Biology, Chemistry, and Engineering* (Addison-Wesley, Reading, MA, 1994).

[46] These two models are related by a variable substitution.

[47] G. Filatrella, N. F. Pedersen, and K. Wiesenfeld, Phys. Rev. E **75**, 017201 (2007); F. Giannuzzi, D. Marinazzo, G. Nardulli, M. Pellicoro, and S. Stramaglia, *ibid.* **75**, 051104 (2007).

[48] H. Daido, Prog. Theor. Phys. **88**, 1213 (1992); **89**, 929 (1993); J. Phys. A **28**, L151 (1995); Phys. D (Amsterdam) **91**, 24 (1996).